

---

# Errors-in-Variables for deep learning: rethinking aleatoric uncertainty

---

Jörg Martin\*, Clemens Elster\*

## Abstract

We present a Bayesian treatment for deep regression using an Errors-in-Variables model which accounts for the uncertainty associated with the input to the employed neural network. It is shown how the treatment can be combined with already existing approaches for uncertainty quantification that are based on variational inference. Our approach yields a decomposition of the predictive uncertainty into an aleatoric and epistemic part that is more complete and, in many cases, more consistent from a statistical perspective. We illustrate and discuss the approach along various toy and real world examples.

## 1 Introduction

In this work we will focus on regression problems that describe the supervised training of neural networks with normally distributed data. For motivational purposes let us first consider the following, quite common, model that links input data  $x$  to outputs  $y$ :

$$y = f_{\theta}(x) + \varepsilon_y, \quad (1)$$

where  $f_{\theta}$  is a neural network with parameters  $\theta$  and where  $\varepsilon_y \sim \mathcal{N}(0, \sigma_y^2)$  is some normally distributed noise<sup>1</sup> that disturbs the true label (i.e., value of the regression function)  $f_{\theta}(x)$  corresponding to  $x$ . Learning the neural network means to infer a value for  $\theta$  from pairs  $(x, y)$  contained in a training set  $\mathcal{D}$ . The trained neural network can then be used to make predictions. In real-world applications, especially in those where reliability and safety are crucial [19, 18, 21], it is valuable, if not indispensable, to know the uncertainty behind a prediction.

Uncertainty in machine learning is usually categorized by two different terms. *Epistemic* uncertainty arises from the uncertainty about the trained model, that is about  $\theta$  in the notation of (1). In a Bayesian approach, as in this work, this uncertainty is described by the posterior  $\pi(\theta|\mathcal{D})$ , which is the distribution of  $\theta$  conditional on the data  $\mathcal{D}$  [1, 8, 15]. This type of uncertainty vanishes as the number of observations tends to infinity, as follows for instance from the Bernstein-von Mises theorem. *Aleatoric* uncertainty, on the other hand, describes an uncertainty that is inherent to the data and cannot be diminished even with an infinite training set. In the context of regression this would correspond to a noise such as  $\varepsilon_y$  in (1) and might be measured, for instance, by  $\sigma_y$ .

A neural network trained for the regression model (1) can be used to make a prediction for the output  $y^*$  given some (further) input  $x^*$ . In a Bayesian treatment, this is done in terms of the posterior predictive distribution. For example, mean and standard deviation of that distribution can be taken as an estimate for  $y^*$  and its associated uncertainty. Both the epistemic and the aleatoric part of the uncertainty enter the posterior predictive distribution and will affect the uncertainty quantification – the epistemic part through the uncertainty in the regression function  $f_{\theta}(x^*)$ , and the aleatoric part due to random noise contained in  $y^*$ .

---

\*Physikalisch-Technische Bundesanstalt, Abbestr. 2, 10587 Berlin

<sup>1</sup>The index  $y$  should not be misunderstood as  $\varepsilon_y$  or  $\sigma_y$  being  $y$  dependent, but is supposed to indicate that the noise corresponds to the output. The same is true for  $\varepsilon_x$  and  $\sigma_x$ , which we introduce in (2) below.

In deep learning, the aleatoric uncertainty expressed through  $\sigma_y$  is often given a greater importance and is regarded as measuring inherent, irreducible label ambiguity [5, 11, 13, 14]. However, such a point of view does no longer apply in those regression problems where the goal is the prediction of the regression function  $f_\theta(x^*)$  at some  $x^*$ . In this case only the epistemic uncertainty about the network’s parameter  $\theta$  remains which, in principle, could become arbitrarily small as the training set grows. Furthermore, typically  $x^* = \zeta^* + \varepsilon_x$  contains some noise  $\varepsilon_x$  as well, and one is actually interested in the value of  $f_\theta(\zeta^*)$ . The uncertainty caused by the fact that  $x^*$ , and not  $\zeta^*$ , is observed constitutes an aleatoric part of the uncertainty for the prediction of  $f_\theta(\zeta^*)$  which is neither covered by  $\sigma_y$  nor by the uncertainty of  $\theta$ .

We here attempt to give a more consistent view on these issues and, arguably, a more accurate depiction. In many cases it is a too crude assumption to presume that while  $y$  is deranged by noise,  $x$  is not. Standard estimation procedures such as maximum likelihood or nonlinear least-squares become biased for a regression model of the form (1) when  $x$  is observed with noise [7]. Furthermore, the separate quantification of the aleatoric part of the uncertainty due to the noise of the input is not possible in a model like (1) since the variance  $\sigma_y^2$  also accounts for noise in the output. Following the idea of Errors-in-Variables (EiV), a quite classical concept in statistics [7], we try to resolve these issues by changing (1) to

$$x = \zeta + \varepsilon_x, \quad y = f_\theta(\zeta) + \varepsilon_y, \quad (2)$$

where  $\zeta$  denotes the true, but unknown input value. Besides allowing for noisy input data, the model (2) enables a treatment of aleatoric uncertainty that is more coherent from a statistical perspective. We will refer to (1) instead as the “non-EiV” model throughout this work. An illustration of both approaches can be found in the appendix.

The uncertainty that arises in the EiV model from estimating  $\zeta$  given  $x$  is an aleatoric uncertainty that has to be taken into account whenever predicting  $f_\theta(\zeta)$ . It explains why there can be an uncertainty of the prediction even if there is no epistemic uncertainty left, without forcing this role on the output noise. We will approach (2) from a Bayesian point of view which is a consistent way for describing uncertainty but poses the challenge to sample from a high dimensional posterior on  $\theta$ . To overcome this obstacle, we build on the idea to use variational inference, as e.g. in [1, 8, 9, 15]. In fact our approach is agnostic to the specific form of the variational distribution and could be used to extend any of these works. For convenience the results in Section 3 below were produced with the variational distribution induced by Monte Carlo dropout [8], but let us stress that there is no profound reason for using this approach in this work other than its ease of implementation. In fact, studying how well different methods perform under EiV could be an exciting outlook for future work.

### Existing work and structure of the article

Errors-in-Variables is a statistical concept that is around since decades [10]. The particular idea of fixing the ratio between  $\sigma_x$  and  $\sigma_y$ , which we propose in Section 2.3 below, is also quite classical [7] and occasionally named after Deming [4]. Variational inference is another well-established tool from statistics that is behind much of the deep learning literature on uncertainty quantification [1, 8, 9, 15, 6, 22]. A concept building on variational inference that has some particular resemblance to this work is the one of variational autoencoders [16]: think of  $\zeta$  in (2) to be the “latent variable”. However variational autoencoders differ in their philosophy and their loss function and are therefore not directly comparable to our approach, although combining both ideas might be a way to enhance the model in (2).

This article is structured as follows. In Section 2 we will discuss the generic approach presented in this work, give a proposal for the underlying priors and discuss some details useful for implementation, such as how to link  $\sigma_x$  and  $\sigma_y$  via a Deming factor  $\delta$  to ensure identifiability and prevent overfitting. In Section 3 we discuss the results of some experiments. The focus will be laid on toy models with known ground truth to study the behavior of the EiV model in greater depth.

## 2 An EiV model for deep learning

In this section we will introduce an Errors-in-variables (EiV) model for deep learning, discuss the concept of aleatoric and epistemic uncertainty in the light of this approach and propose a few algorithmic details for training.

## 2.1 The generic model

Suppose we have  $N$  datapoints  $\mathcal{D} = \{(x_1, y_1), \dots, (x_N, y_N)\} \subseteq \mathbb{R}^{n_x} \times \mathbb{R}^{n_y}$  that we model by

$$x_i = \zeta_i + \varepsilon_{x,i}, \quad y_i = f_\theta(\zeta_i) + \varepsilon_{y,i} \quad (3)$$

with normally distributed  $\varepsilon_{x,i} \sim \mathcal{N}(0, \sigma_x^2 I_{n_x \times n_x})$ ,  $\varepsilon_{y,i} \sim \mathcal{N}(0, \sigma_y^2 I_{n_y \times n_y})$  and where the parameters  $\theta \in \mathbb{R}^p$ ,  $\sigma_x, \sigma_y > 0$  and  $\zeta_1, \dots, \zeta_N \in \mathbb{R}^{n_x}$  are unknown. The function  $f_\theta$  will be a neural network. The  $\zeta_i$  ought to be considered as the true, but unknown, inputs we would like to feed to  $f_\theta$ . Given  $\zeta = (\zeta_1, \dots, \zeta_N)$ ,  $\theta$  and  $\sigma^2 = (\sigma_x^2, \sigma_y^2)$ , the likelihood for the data  $\mathcal{D}$  under (3) is

$$p(\mathcal{D}|\theta, \zeta, \sigma^2) = \prod_{i=1}^N p(x_i|\zeta_i, \sigma_x^2) \cdot p(y_i|\theta, \zeta_i, \sigma_y^2) \quad (4)$$

with  $p(x_i|\zeta_i, \sigma_x^2) = \mathcal{N}(x_i|\zeta_i, \sigma_x^2)$  and  $p(y_i|\theta, \zeta_i, \sigma_y^2) = \mathcal{N}(y_i|f_\theta(\zeta_i), \sigma_y^2)$ . While  $\theta$  will be considered as the parameter of interest, the  $\zeta$  will be considered as nuisance parameters and the variances in  $\sigma^2$  as hyperparameters that will be finetuned, learned or chosen from experience. Fixing a prior  $\pi(\theta, \zeta) = \pi(\theta)\pi(\zeta) = \pi(\theta) \prod_{i=1}^N \pi(\zeta_i)$  we have, by Bayes' theorem,

$$\pi(\theta|\mathcal{D}, \sigma^2) = \frac{\pi(\theta)\pi(\mathcal{D}|\theta, \sigma^2)}{\pi(\mathcal{D}|\sigma^2)}, \quad (5)$$

where  $\pi(\mathcal{D}|\sigma^2) = \int d\theta \pi(\theta)\pi(\mathcal{D}|\theta, \sigma^2)$  and, due to (4) and once more Bayes' theorem,

$$\pi(\mathcal{D}|\sigma^2) = \int d\zeta \pi(\zeta) p(\mathcal{D}|\theta, \zeta, \sigma^2) = \prod_{i=1}^N \pi(x_i|\sigma_x^2) \int d\zeta_i \pi(\zeta_i|x_i, \sigma_x^2) p(y_i|\zeta_i, \theta, \sigma_y^2) \quad (6)$$

with  $\pi(x_i|\sigma_x^2) = \int d\zeta_i \pi(\zeta_i) p(x_i|\zeta_i, \sigma_x^2)$ . As we do not expect  $\pi(\theta|\mathcal{D}, \sigma^2)$  to be feasible we approximate it via a variational distribution

$$\pi(\theta|\mathcal{D}, \sigma^2) \approx q_\phi(\theta) \quad (7)$$

with variational parameter  $\phi$ . In variational inference the distance in (7) is measured by the Kullback-Leibler divergence  $D_{\text{KL}}(q_\phi(\theta)\|\pi(\theta|\mathcal{D}, \sigma^2))$ . Using that the divergence is non-negative, (5) and (6) we obtain the following evidence lower bound (ELBO) for the data evidence  $\log \pi(\mathcal{D}|\sigma^2)$

$$\begin{aligned} \text{ELBO} &= \sum_{i=1}^N \int d\theta q_\phi(\theta) \log \left( \int d\zeta_i \pi(\zeta_i|x_i, \sigma_x^2) p(y_i|\theta, \zeta_i, \sigma_y^2) \right) \\ &\quad - D_{\text{KL}}(q_\phi(\theta)\|\pi(\theta)) + \sum_{i=1}^N \log \pi(x_i|\sigma_x^2) \leq \log \pi(\mathcal{D}|\sigma^2). \end{aligned} \quad (8)$$

Setting  $\mathcal{L}(\phi, \sigma^2) = -\text{ELBO}$  we then want to find  $\phi, \sigma_x^2, \sigma_y^2$  so that

$$\phi, (\sigma_x^2, \sigma_y^2) = \arg \min_{\phi, \sigma^2} \mathcal{L}(\phi; \sigma^2). \quad (9)$$

In optimizing  $\phi$  and the hyperparameters  $\sigma^2$  at the same time we here follow a common scheme, cf. [16]. To solve (9), we use backpropagation on the following Monte-Carlo object

$$\begin{aligned} \mathcal{L}^{\text{M.C.}}(\phi; \sigma^2) &:= -\frac{1}{M} \sum_{m=1}^M \log \left( \frac{1}{L} \sum_{l=1}^L p(y_{i_m}|\theta_m, \zeta_{i_m,l}, \sigma_y^2) \right) \\ &\quad + \frac{1}{N} D_{\text{KL}}(q_\phi(\theta)\|\pi(\theta)) - \frac{1}{M} \sum_{m=1}^M \log \pi(x_{i_m}|\sigma_x^2), \end{aligned} \quad (10)$$

where the minibatches  $\{(x_{i_1}, y_{i_1}), \dots, (x_{i_M}, y_{i_M})\}$ , the  $M$  samples  $\theta_m \sim q_\phi(\theta_m)$  and  $M \cdot L$  samples  $\zeta_{i_m,l} \sim \pi(\zeta_{i_m,l}|x_{i_m}, \sigma_x^2)$  will be drawn anew in each optimization step. Note that the way  $\theta_m$  is sampled in (10) differs slightly from the way this is done in approaches such as [8, 9, 15] as  $\theta_m$  will be identical for all inputs  $\zeta_{i_m,l}$  with the same  $m$ .<sup>2</sup> For some algorithms on the other hand, such as Bayes by Backprop [1], taking in (10) a single Monte Carlo sample  $\theta_m = \theta$  for all  $m$  instead might allow for a more efficient implementation. The loss function in (8) and (10) is the backbone of the EiV algorithm. To make the first term in (10) numerically stable, and suitable for backpropagation, the common "logsumexp" function can be used. Before we can use (10) for training however, we still have to fix the prior distributions and the variational distribution  $q_\phi$ .

<sup>2</sup>For the approach from [15] this also means that Gaussian dropout of "type A" has to be used.

## 2.2 Choosing $\pi(\theta)$ , $\pi(\zeta_i)$ and $q_\phi$

Choosing  $\pi(\theta)$  is rather standard in the literature on Bayesian neural networks and complies with choosing a regularization for  $\theta$ , cf. [1]. We will here follow the common choice of a centered normal distribution  $\pi(\theta) = \mathcal{N}(\theta|0, \lambda_\theta^2)$ , that formally corresponds to an  $L^2$  regularization.

The prior  $\pi(\zeta_i)$  is more particular to the EiV approach. If we consider for instance images as the inputs to our neural network a natural choice would be to consider a distribution whose bulk covers the pixel range. For the choice  $\pi(\zeta_i) = \mathcal{N}(\zeta_i|0, \lambda_\zeta^2)$  we obtain

$$\pi(\zeta_i|x_i, \sigma_x^2) = \mathcal{N}\left(\zeta_i \left| \left(1 + \frac{\sigma_x^2}{\lambda_\zeta^2}\right)^{-1} x_i, \left(1 + \frac{\sigma_x^2}{\lambda_\zeta^2}\right)^{-1} \sigma_x^2\right.\right), \quad \pi(x_i|\sigma_x^2) = \mathcal{N}(x_i|0, \sigma_x^2 + \lambda_\zeta^2). \quad (11)$$

In Section 3 we will use the constant, improper, prior that arises for  $\lambda_\zeta \rightarrow \infty$ . In this limit the marginal  $\pi(x_i|\sigma_x^2)$  is obviously ill-defined. However, this is not really a problem, since

- $\pi(\zeta_i|x_i, \sigma_x^2) \xrightarrow{\lambda_\zeta \rightarrow \infty} \mathcal{N}(\zeta_i|x_i, \sigma_x^2)$  is well-defined and can be sampled from
- The divergence of  $\prod_i \pi(x_i|\sigma_x^2)$  that appears in (6) cancels out in (5), so that there is a proper posterior  $\pi(\theta|\mathcal{D}, \sigma^2)$  in the limit.
- The only non-convergent term of  $-\mathcal{L}(\phi, \sigma^2)$  for  $\lambda_\zeta \rightarrow \infty$  is given by  $\frac{1}{N} \sum_{i=1}^N \log \pi(x_i|\sigma_x^2) = -\frac{1}{N} \sum_{i=1}^N \frac{x_i^2}{2(\sigma_x^2 + \lambda_\zeta^2)} - \frac{1}{2} \log(2\pi(1 + \frac{\sigma_x^2}{\lambda_\zeta^2})) - \log \lambda_\zeta$  or, more precisely, by its term  $-\log \lambda_\zeta$  that can be dropped as it does not depend on  $\phi$  or  $\sigma^2$ .

The choice of  $q_\phi$  is only limited by three requirements. First of all, we need to be able to sample from  $q_\phi$ . Secondly, we need an expression for the regularizer  $D_{\text{KL}}(q_\phi(\theta) \parallel \pi(\theta))$  - either explicitly or via Monte Carlo Sampling [16]. Finally, we have to be able to optimize the arising loss function  $\mathcal{L}(\phi, \sigma^2)$  w.r.t.  $\phi$  for example via the reparametrization trick [16]. Merely for convenience we will restrict ourselves in this work to the popular choice of Monte Carlo dropout [8] where  $q_\phi$  arises from dropping randomly nodes of the network with some probability and where  $\phi$  simply coincides with the network parameters. However, let us emphasize that the algorithm described in this work is by no means restricted to this particular choice but is usable for any  $q_\phi$  for which the above applies.

## 2.3 Algorithmic details

In total our algorithm, that implements the optimization (9), is optimizing three objects  $\phi$ ,  $\sigma_x$  and  $\sigma_y$ . While  $\phi$  and  $\sigma_y$  can be optimized as in the corresponding non-EiV model, the optimization w.r.t  $\sigma_x$  needs some discussion. Using (11) this optimization can be implemented via the reparametrization trick and is influenced by the chosen  $\lambda_\zeta$ . If we let  $\lambda_\zeta \rightarrow \infty$  as described in Subsection 2.2 we found, for the examples from Section 3, that the optimization (9) often led to vanishing  $\sigma_x$ .<sup>3</sup> To prevent this from happening, we here propose, at least for large or infinite  $\lambda_\zeta$  to use the Deming regression [4], that is

$$\sigma_x = \delta \cdot \sigma_y. \quad (12)$$

We will dub in this work  $\delta$  the *Deming factor* and keep it fixed during training. By choosing  $\delta$  the impact of the input noise can be controlled. For data that is normalized in both, input and output, choosing  $\delta = 1$  might be a reasonable choice when one expects input and output to be noisy whereas for  $\delta \searrow 0$  the impact of the input noise in the EiV model is diminished and the non-EiV model is recovered. A strategy to estimate the best  $\delta$  for a given dataset would be the content of a work on its own; nevertheless we will give a small discussion in Section 3 below. Practically, (12) means that when learning  $\sigma^2 = (\sigma_x^2, \sigma_y^2)$  we only have to learn one of its components. In this work we learn  $\sigma_y^2$  and compute  $\sigma_x^2$  from (12).

When training  $\phi$  and  $\sigma_y^2$  using (12) we found the following splitting effective in producing better results on both parameters: split the number of training epochs  $n_{\text{train}}$  in three parts  $n_{\text{train}} = n_{\text{only } \phi} +$

<sup>3</sup>At least when looking at the maximum likelihood solution of the EiV model (3) this behavior appears sensible as the likelihood becomes infinite for  $\sigma_x = 0$  and  $\zeta_i = x_i$  if there are no "duplicate"  $x_i$  with different labels in the data.

$n_{\text{increase } \delta} + n_{\text{fine-tune}}$ . Starting from some initial values for  $\phi$  and  $\sigma_y^2$  and with Deming factor  $\tilde{\delta} = 0$  only update  $\phi$  via (10) for  $n_{\text{only } \phi}$  epochs. Thereafter, for  $n_{\text{increase } \delta}$  epochs, starting from 0, increase  $\tilde{\delta}$  before each epoch by  $\delta/n_{\text{increase } \delta}$  and then train  $\phi$  and  $\sigma_y^2$ . Finally, train  $\phi$  and  $\sigma_y^2$  using the full Deming factor  $\tilde{\delta} = \delta$  for  $n_{\text{fine-tune}}$  epochs. The full algorithm is summarized in the appendix.

## 2.4 A new view on aleatoric uncertainty

Once the neural network is trained the learned  $\phi$  and  $\sigma^2$  can be used to obtain uncertainties and predictions for a new  $x^*$ . Namely, we draw  $\zeta^*$  from<sup>4</sup>  $\pi(\zeta^*|x^*, \sigma_x^2) = \pi(\zeta^*|x^*, \mathcal{D}, \sigma_x^2)$  and  $\theta$  from  $q_\phi(\theta)$  and use the distribution of the regression curve  $f_\theta(\zeta^*)$ . To express predictions and uncertainties, we can then either use quantiles or moments. For the latter we set

$$m(x^*) = \mathbb{E}_{\substack{\theta \sim \pi(\theta|\mathcal{D}, \sigma^2), \\ \zeta^* \sim \pi(\zeta^*|x^*, \sigma_x^2)}} [f_\theta(\zeta^*)], \quad u(x^*)^2 = \text{Var}_{\substack{\theta \sim \pi(\theta|\mathcal{D}, \sigma^2), \\ \zeta^* \sim \pi(\zeta^*|x^*, \sigma_x^2)}} [f_\theta(\zeta^*)], \quad (13)$$

where the uncertainty  $u(x^*)$  can be split into (law of total variance)

$$\begin{aligned} u(x^*)^2 &= \mathbb{E}_{\zeta^* \sim \pi(\zeta^*|x^*, \sigma_x^2)} (\text{Var}_{\theta \sim \pi(\theta|\mathcal{D}, \sigma^2)} [f_\theta(\zeta^*)]) && \text{(epistemic)} \\ &+ \text{Var}_{\zeta^* \sim \pi(\zeta^*|x^*, \sigma_x^2)} (\mathbb{E}_{\theta \sim \pi(\theta|\mathcal{D}, \sigma^2)} [f_\theta(\zeta^*)]). && \text{(aleatoric)} \end{aligned} \quad (14)$$

The detailed algorithm on how to compute  $m(x^*)$  and  $u(x^*)$  is contained in the appendix.

The ‘‘classical’’ treatment of epistemic and aleatoric uncertainty, based on the posterior predictive and discussed in Section 1, can be easily combined with the above. For the posterior predictive  $\pi(y^*|x^*, \mathcal{D}, \sigma^2)$ , we draw for each sample  $f_\theta(\zeta^*)$  labels  $y^*$  from  $\mathcal{N}(f_\theta(\zeta^*), \sigma_y^2)$ . The variance of this distribution can then be split into

$$\text{Var}_{y^* \sim \pi(y^*|x^*, \mathcal{D}, \sigma^2)} [y^*] = u(x^*)^2 + \sigma_y^2 \quad (15)$$

and is therefore simply augmented by an extra term  $\sigma_y^2$ . For  $\sigma_x \searrow 0$  the aleatoric part of  $u(x^*)$  in (14) vanishes,  $u(x^*)$  coincides with the epistemic uncertainty and (15) morphs into the ‘‘classical’’ split in aleatoric and epistemic uncertainty. The usage of the aleatoric part  $\sigma_y^2$  that appears in (15) as an uncertainty is only justified if one is really interested in the uncertainty of a noise perturbed label  $y^*$  given  $x^*$ . If one is actually interested in the ground truth predicted by  $f_\theta(\zeta^*)$  (EiV) or  $f_\theta(x^*)$  (non-EiV) than it is inappropriate to take the second term in (15) into account.

By introducing an additional aleatoric uncertainty in (14) the EiV model introduces an aleatoric uncertainty that is still consistent with statistics in such cases. In fact as we will see in Figure 1 below, for increasing Deming factor  $\delta$  part of the uncertainty previously captured by  $\sigma_y$  gets transferred to the input uncertainty that is captured by  $\sigma_x$ . The second term of (14) not only provides an aleatoric uncertainty that is still available if considering the ground truth predicted by  $f_\theta$ , but in addition exploits a source of uncertainty that is not present in the non-EiV model and thus gives a more complete description of reality. Finally, by distinguishing between  $\zeta^*$  and  $x^*$  the EiV model introduces a new concept of prediction, cf. (13), that differs from the non-EiV model.

## 3 Experiments

For evaluating the model introduced in Section 2 we used four datasets, where two were generated with a known ground truth and two are real world examples. To keep the setup as lucid as possible and to avoid anisotropic issues, we here only consider datasets with 1-dimensional labels  $y$ . For all datasets, we used the  $q_\phi$  induced by Bernoulli dropout [8] with a dropout rate of 0.5. Training both, EiV and non-EiV, alongside each other with the same  $q_\phi$  allows us to judge the quality of our EiV model and serves as a consistency check as we expect the EiV model to behave like the non-EiV model for small Deming factors,  $\delta \searrow 0$ . The training time for all datasets is slightly increased by the EiV method due to the multiple sampling of  $\zeta$  in (10) but is of comparable magnitude. Using a single Tesla K80 GPU a training run of both models took a few minutes for the examples below, with exception of the multinomial example where the training time was around an hour for both models. All experiments were implemented in the Python library PyTorch [20] (BSD license).

<sup>4</sup>Note that we understand  $\zeta^*$  as independent of the  $\zeta_i$  that generated the  $x_i$  and  $y_i$  in  $\mathcal{D}$ , which is why we can drop the conditioning on  $\mathcal{D}$ .

Table 1: Results of the non-EiV model and the EiV model for those datasets from Section 3 with known ground truth, varying  $\tilde{\sigma}_x$  and Deming factors  $\delta = 0.15$  (for  $\tilde{\sigma}_x=0.05$ ), 0.20 (for  $\tilde{\sigma}_x=0.07$ ) and 0.30 (for  $\tilde{\sigma}_x=0.10$ ). The RMSE is w.r.t. noisy data (and not the ground truth). The second column denotes the coverage of the ground truth by the uncertainty times 1.96. All results were averaged over 20 different training runs and different random seeds. The displayed digits are certain w.r.t. the corresponding standard errors.

data		Mexican hat			multinomial		
$\sigma_x$		0.05	0.07	0.10	0.05	0.07	0.10
RMSE	EiV	0.34	0.35	0.38	0.67	0.76	0.85
	non-EiV	0.34	0.36	0.38	0.63	0.71	0.80
coverage	EiV	0.97	0.93	0.91	0.96	0.92	0.79
	non-EiV	0.90	0.82	0.72	0.80	0.63	0.42

First we will consider the problem of fitting a one-dimensional ‘‘Mexican hat’’  $g(\zeta) = (1 - (4\zeta)^2)e^{-\frac{1}{2}(4\zeta)^2}$ , compare the blue line in Figure 2a.

We drew 300 values for  $\zeta$  uniformly between -1 and 1, computed the corresponding  $g(\zeta)$  and disturbed  $\zeta$  and  $g(\zeta)$  by Gaussian noise with standard deviations  $\tilde{\sigma}_x = 0.05, 0.07, 0.10$  and  $\tilde{\sigma}_y = 0.30$ . For each choice of  $\tilde{\sigma}_x$  and various choices of the Deming factor  $\delta$  (cf. Figure 1) a fully connected neural network with 3 hidden layers (50, 100 and 50 neurons) was trained, both with and without EiV. With the notation of Section 2.3 we used  $n_{\text{train}} = 1000$  with  $n_{\text{only } \phi} = 300$  and, for the EiV models,  $n_{\text{increase } \delta} = 20$ . For the last 50 of the 1000 training epochs the learning rate was decreased from  $10^{-3}$  to  $10^{-4}$ .

Figure 1 shows the evolution of  $\sigma_y$  during training for the non-EiV model and the EiV model for all studied Deming factors and  $\tilde{\sigma}_x = 0.07$  for 20 training runs. For small  $\delta$  the evolution of  $\sigma_y$  for the EiV model and the non-EiV are essentially identical. For increasing  $\delta$  the learned value of  $\sigma_y$  decreases as  $\sigma_x = \delta \cdot \sigma_y$  is more and more used to capture the noise of the data. However, for all chosen values we see that after training we obtain  $\sigma_y > \tilde{\sigma}_y$  (dotted, blue), which is natural as we expect the learned  $\sigma_y$  to partially include the model misfit. We thus expect the optimal choice of  $\delta$  to be slightly below the quotient  $\frac{\tilde{\sigma}_x}{\tilde{\sigma}_y}$ .

Figure 2 shows the prediction of an EiV model with  $\delta = 0.2$ , which is slightly below  $\frac{\tilde{\sigma}_x}{\tilde{\sigma}_y}$ , and a non-EiV model, both trained on input data with  $\tilde{\sigma}_x = 0.07$ . Considering errors in the input has the interesting consequence that we can compare two kind of predictions, which are shown in Figure 2a and 2b. In both Figures the blue curve shows the ground truth  $g(\zeta)$ . Figure 2a compares  $\mathbb{E}_{\theta \sim q_\phi(\theta)}[f_\theta(\zeta)]$  of the EiV model (red) and the non-EiV model (black). The red and black areas mark 1.96 times the standard deviation of  $f_\theta(\zeta)$  when drawing  $\theta$  from  $q_\phi(\theta)$ . In practice, however,  $\zeta$  is unknown and all we see is a noisy  $x \sim p(x|\zeta, \tilde{\sigma}_x^2)$ . This case is depicted in Figure 2b. For each  $\zeta$  we drew a  $x \sim p(x|\zeta, \tilde{\sigma}_x^2)$  and then computed  $\mathbb{E}_{\theta \sim q_\phi(\theta)}[f_\theta(x)]$  for the non-EiV model and  $m(x)$  as in (13) for the EiV model. The black area depicts once more 1.96 times the epistemic uncertainty, while the red one now represents 1.96 times  $u(x)$  of (13).

Figure 2a shows that the epistemic uncertainty of the EiV model and non-EiV evaluated on  $\zeta$  are pretty comparable with only slight differences. In Figure 2b we observe larger uncertainties for

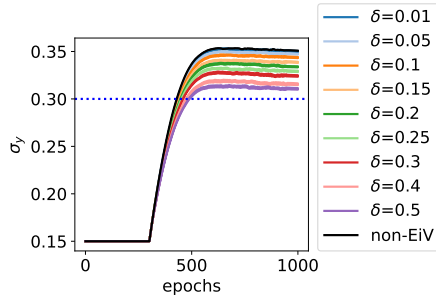


Figure 1: The learned  $\sigma_y$  during training for the non-EiV model and the EiV model with varying Deming factor  $\delta$  for data around a Mexican hat curve and 20 training runs. The plotted areas depict one standard error around the average. The  $\tilde{\sigma}_y$  used for generating the data is marked by the blue, dashed line. A larger Deming factor lets the final  $\sigma_y$  decrease by explaining more of the noise via input uncertainty. For  $\delta \searrow 0$  EiV and non-EiV coincide.

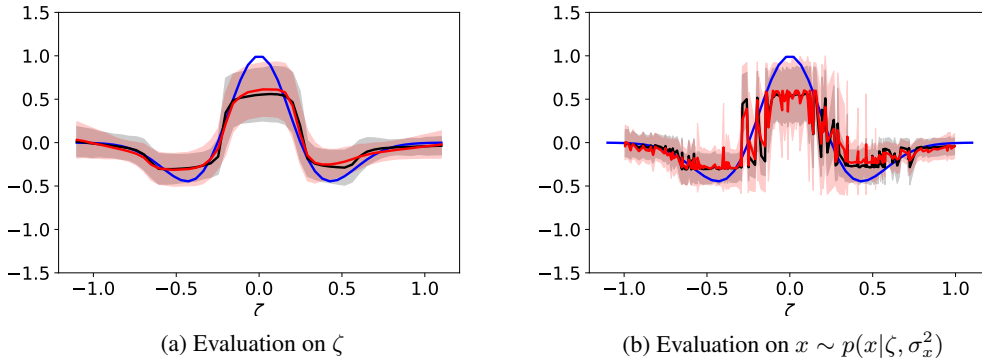


Figure 2: Predictions and uncertainties of a non-EiV model (black) and an EiV model (red,  $\delta = 0.2$ ), trained on data around a Mexican hat (blue) that was disturbed by noise with  $\tilde{\sigma}_x = 0.07$ ,  $\tilde{\sigma}_y = 0.3$ . On the left the models are evaluated on “true”  $\zeta$  and on the right on noisy  $x \sim p(x|\zeta, \tilde{\sigma}_x^2)$ . Predictions and uncertainties are computed as described in Section 3.

the EiV model. Due to the random nature of the plot it is however hard to perceive if these larger uncertainties are necessary for a better coverage of the ground truth. The plot in Figure 3 reveals that this is indeed the case. It shows for each  $\zeta$  the coverage, under repeated sampling of  $x \sim \pi(\zeta|x, \tilde{\sigma}_x^2)$ , of the ground truth  $g(\zeta)$  by the intervals  $m(x) \pm 1.96 u(x)$  for the EiV model (red) and  $\mathbb{E}_{\theta \sim q_{\phi}(\theta)}[f_{\theta}(x)] \pm 1.96 \text{Var}_{\theta \sim q_{\phi}(\theta)}(f_{\theta}(x))^{1/2}$  for the non-EiV model (black). The dots and bars in Figure 3 mark the mean of the coverage and its standard error under 20 different training runs and random seeds. The dashed, blue line marks 0.95. We see that with the exception of the peak of the Mexican hat, which both models fail to capture correctly, the EiV model has a substantially better coverage of the ground truth. The middle column of Table 1 summarizes the coverage for all considered choices of  $\tilde{\sigma}_x$ . Table 1 also shows the root mean squared error (RMSE) of the prediction  $m(x)$  (EiV), as in (13), and of  $\mathbb{E}_{\theta \sim q_{\phi}(\theta)}[f_{\theta}(x)]$  (non-EiV) w.r.t. the noisy data. Note that while the RMSE is almost identical for EiV and non-EiV the coverage is substantially improved by considering Errors-in-Variables. The results in Table 1 were averaged over 20 training runs and are specified with those digits that are certain under the corresponding standard error.

The right column “multinomial” of Table 1 shows the according results for another example created with a 5D polynomial with random coefficients that was multiplied by  $e^{-\sin(5|\zeta|^2)}$ . We used the same choices of  $\tilde{\sigma}_x$ ,  $\tilde{\sigma}_y$  and  $\delta$  as above and once more a fully connected neural networks with three hidden layers (500, 300 and 100 neurons). Figure 4 shows, as in Figure 2b, the predictions and uncertainties for  $x \sim p(x|\zeta, \tilde{\sigma}_x^2)$  drawn for  $\zeta$  along one axis. The results of Table 1 show once more that the EiV model produces a similar, only slightly increased, RMSE compared to the non-EiV model but a substantially better coverage with its uncertainties.

While examples with a known ground truth are useful to judge quantities such as the epistemic uncertainty or (14), in practice the noise-free ground truth will usually be unknown, even for the training data. As two final examples we will therefore study two real world examples, where no ground truth is available and which are available as open datasets. We consider the prediction of the quality of Portuguese red “Vinho Verde” [2], that contains for each of the 1599 studied wines a quantity quantifying the quality and 11 chemical properties as well as the Boston Housing dataset [12]. For the first dataset all concentrations were transformed by a logarithm and the inputs and output were normalized to have mean 0 and standard deviation 1. A subset of 20% was split off for testing purposes. On the remaining a fully connected neural network with three hidden layers (with 200, 100 and 50 neurons) was trained with various choices of Deming factors  $\delta$  for 400 epochs. On the second dataset the disputed [3] 12th column was removed, inputs and output were normalized and a subset of 20% was split off for testing. On the remainder a fully connected neural network with three hidden layers (200, 100 and 50 neurons) was trained for 1000 epochs. Figure 5 shows the average of the RMSE, together with its standard error, on the test set depending on the used  $\delta$  for 20 training runs with different random seeds for both datasets. For the non-EiV model the area of one standard error around the mean is depicted in gray. We saw already in Table 1 that the RMSE cannot be used as a sole measure to judge the quality of the used model: a slightly worse RMSE can

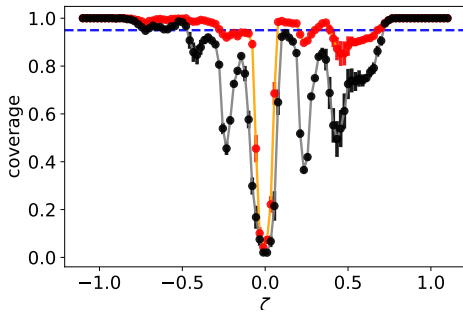


Figure 3: The coverage of the ground truth by the uncertainty (times 1.96) for the EiV model (red-orange,  $\delta = 0.2$ ) and the non-EiV model (black-gray) as in Figure 2b for the Mexican hat with  $\tilde{\sigma}_x = 0.07$ , under repeated sampling of  $x \sim p(x|\zeta, \tilde{\sigma}_x^2)$ . The plot shows the averages (dots) and its standard errors (bars) over 20 training runs with different random seeds. The dashed, blue line marks 0.95.

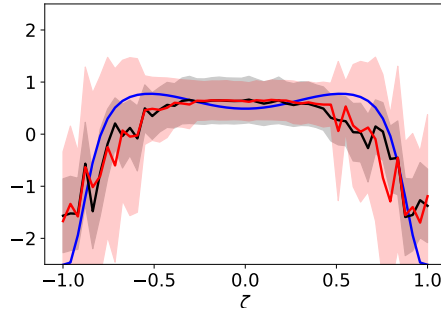
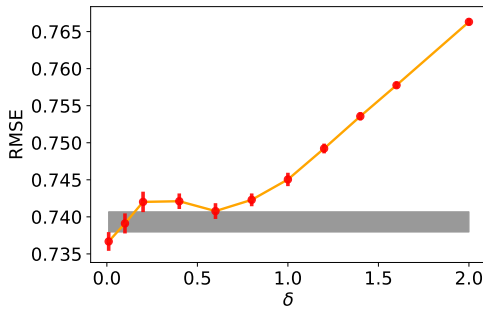
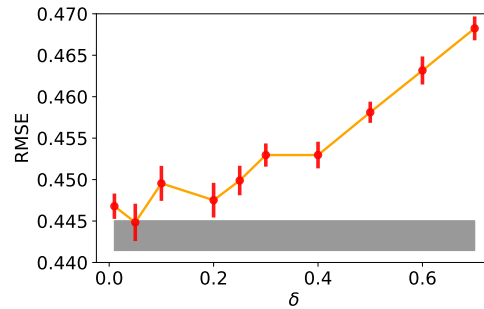


Figure 4: Predictions and uncertainties of a non-EiV model (black) and an EiV model (red,  $\delta = 0.2$ ) for data following a modulated 5D polynomial (blue) with  $\tilde{\sigma}_x = 0.07, \tilde{\sigma}_y = 0.30$  along one axis when evaluating the model on  $x \sim p(x|\zeta, \tilde{\sigma}_x^2)$ . Predictions and uncertainties are computed as described in Section 3.



(a) Wine quality



(b) Boston Housing

Figure 5: Dependency of the RMSE of the EiV model on the Deming factor  $\delta$  from (12) for the Wine quality and Boston Housing dataset for 20 training runs and different random seeds. The plot shows the means (dots) and its standard errors (bars). For the non-EiV model the range of the standard error around the mean is depicted by the gray area.

come with a much better uncertainty coverage. However, studying the RMSE can help to rule out too large values for  $\delta$  that lead to a bad fit and overprudent small  $\delta$ . From Figure 5a a good choice for the wine quality dataset might be  $\delta = 0.6$  with a relatively small RMSE. The “symmetric” choice  $\delta = 1$  (with  $\sigma_x = \sigma_y$ ) on the other hand yields only a slightly worse RMSE as the non-EiV model. In fact, as we can see in Figure 6a the errors that both models make for  $\delta = 1$  are almost identical. The uncertainty, on the other hand, depicted in Figure 6b, is increased for the EiV model. This is identical to the behavior observed for the toy examples in Figure 2b and 4. As we have no ground truth available for this dataset a coverage as in Table 1 cannot be computed.

## 4 Conclusion and discussion

We showed how Errors-in-Variables (EiV), a classical concept from statistics, can be combined with existing Bayesian methods for uncertainty quantification in deep regression. This not only allows to treat the input of the network as equipped with an uncertainty but also gives a notion of aleatoric uncertainty that is more coherent with statistics. We found this method to give predictions of a similar quality as the non-EiV method but with an increased uncertainty. For examples with known

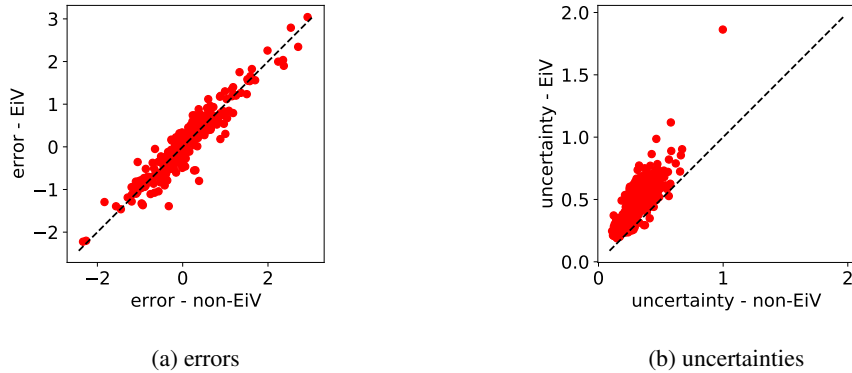


Figure 6: The deviation of the prediction from the label  $y$  (left) and the uncertainty (right) for test datapoints from the wine quality dataset [2] for the EiV model ( $y$ -axis,  $\delta = 1$ ) and the non-EiV model ( $x$ -axis). The dashed, black lines show the diagonals.

ground truth and noisy input this increased uncertainty was observed to be necessary to achieve a better coverage of the ground truth.

The aim of this work is to propose a comparably simple and effective way to treat uncertain input in deep learning, and thereby to allow reconsidering the concept of aleatoric uncertainty. In cases where safety is relevant, e.g. in medical applications, the question whether to doubt or trust a prediction can easily get an ethical dimension. For this reason let us emphasize that, hitherto, all existing uncertainty methods for neural networks, including the one presented in this work, are approximations. Using them blindly might lead to overconfident trust in predictions and thereby to negative individual or societal consequences. A sustainable usage of these methods will require wariness and future research to understand their limits and possible improvements. Concerning this work let us recall some aspects that we encourage to be studied in future work. For instance, to keep the setup simple we restricted ourselves to the variational inference based on Bernoulli dropout. Analyzing how different approaches will impact or perform under Errors-in-Variabes and examining a larger variety of datasets would make a natural follow-up study to this article. The same is true for an enhancement of the distributions involved in (2), which could for instance involve an anisotropic or heteroscedastic adaption or the usage of a learnable push-forward mapping. Finally, our model could further be enhanced by a criterion that allows for a good choice of the Deming factor from (12) or by an approach that replaces the latter by something more sophisticated.

## References

- [1] BLUNDELL, C., CORNEBISE, J., KAVUKCUOGLU, K., AND WIERSTRA, D. Weight uncertainty in neural network. In *International Conference on Machine Learning* (2015), PMLR, pp. 1613–1622.
- [2] CORTEZ, P., CERDEIRA, A., ALMEIDA, F., MATOS, T., AND REIS, J. Modeling wine preferences by data mining from physicochemical properties. *Decision support systems* 47, 4 (2009), 547–553.
- [3] CRANGLE, C. Inadvertent racism in popular data science data set. available at <https://www.linkedin.com/pulse/its-time-retire-boston-housing-dataset-colleen-e-crangle>. Accessed: 2021-05-17.
- [4] DEMING, W. E. Statistical adjustment of data.
- [5] DEPEWEG, S., HERNANDEZ-LOBATO, J.-M., DOSHI-VELEZ, F., AND UDLUFT, S. Decomposition of uncertainty in bayesian deep learning for efficient and risk-sensitive learning. In *International Conference on Machine Learning* (2018), PMLR, pp. 1184–1193.
- [6] DUVENAUD, D., MACLAURIN, D., AND ADAMS, R. Early stopping as nonparametric variational inference. In *Artificial Intelligence and Statistics* (2016), PMLR, pp. 1070–1077.
- [7] FULLER, W. A. *Measurement error models*, vol. 305. John Wiley & Sons, 2009.

- [8] GAL, Y., AND GHAHRAMANI, Z. Dropout as a bayesian approximation: Representing model uncertainty in deep learning. In *international conference on machine learning* (2016), PMLR, pp. 1050–1059.
- [9] GAL, Y., HRON, J., AND KENDALL, A. Concrete dropout. *arXiv preprint arXiv:1705.07832* (2017).
- [10] GILLARD, J. An historical overview of linear regression with errors in both variables. *Math. School, Cardiff Univ., Wales, UK, Tech. Rep* (2006).
- [11] GUSTAFSSON, F. K., DANELLJAN, M., AND SCHON, T. B. Evaluating scalable bayesian deep learning methods for robust computer vision. In *Proceedings of the IEEE/CVF Conference on Computer Vision and Pattern Recognition Workshops* (2020), pp. 318–319.
- [12] HARRISON JR, D., AND RUBINFELD, D. L. Hedonic housing prices and the demand for clean air. *Journal of environmental economics and management* 5, 1 (1978), 81–102.
- [13] HÜLLERMEIER, E., AND WAEGEMAN, W. Aleatoric and epistemic uncertainty in machine learning: An introduction to concepts and methods. *Machine Learning* 110, 3 (2021), 457–506.
- [14] KENDALL, A., AND GAL, Y. What uncertainties do we need in bayesian deep learning for computer vision? *arXiv preprint arXiv:1703.04977* (2017).
- [15] KINGMA, D. P., SALIMANS, T., AND WELLING, M. Variational dropout and the local reparameterization trick. *arXiv preprint arXiv:1506.02557* (2015).
- [16] KINGMA, D. P., AND WELLING, M. Auto-encoding variational bayes. *arXiv preprint arXiv:1312.6114* (2013).
- [17] LENAIL, A. Nn-svg: Publication-ready neural network architecture schematics. *Journal of Open Source Software* 4, 33 (2019), 747.
- [18] LITJENS, G., KOOI, T., BEJNORDI, B. E., SETIO, A. A. A., CIOMPI, F., GHAFOORIAN, M., VAN DER LAAK, J. A., VAN GINNEKEN, B., AND SÁNCHEZ, C. I. A survey on deep learning in medical image analysis. *Medical image analysis* 42 (2017), 60–88.
- [19] MCALLISTER, R., GAL, Y., KENDALL, A., VAN DER WILK, M., SHAH, A., CIPOLLA, R., AND WELLER, A. Concrete problems for autonomous vehicle safety: Advantages of bayesian deep learning. International Joint Conferences on Artificial Intelligence, Inc.
- [20] PASZKE, A., GROSS, S., CHINTALA, S., CHANAN, G., YANG, E., DEVITO, Z., LIN, Z., DESMAISON, A., ANTIGA, L., AND LERER, A. Automatic differentiation in pytorch. In *NIPS-W* (2017).
- [21] SÜNDERHAUF, N., BROCK, O., SCHEIRER, W., HADSELL, R., FOX, D., LEITNER, J., UPCROFT, B., ABBEEL, P., BURGARD, W., MILFORD, M., ET AL. The limits and potentials of deep learning for robotics. *The International Journal of Robotics Research* 37, 4-5 (2018), 405–420.
- [22] ZHANG, G., SUN, S., DUVENAUD, D., AND GROSSE, R. Noisy natural gradient as variational inference. In *International Conference on Machine Learning* (2018), PMLR, pp. 5852–5861.

## 5 Appendix

**Data:** Training data  $\mathcal{D} = \{(x_1, y_1), \dots, (x_N, y_N)\}$

**Result:**  $\phi$  and  $\sigma^2$

Fix  $\pi(\zeta), \pi(\theta), \delta$ ;

Choose initial  $\phi$  and  $\sigma_y$ ;

Fix  $n_{\text{train}} = n_{\text{only } \phi} + n_{\text{increase } \delta} + n_{\text{fine-tune}}$ ;

```

for  $j$  in  $1, \dots, n_{\text{train}}$  do
  if  $j \leq n_{\text{only } \phi}$  then
     $\tilde{\delta} \leftarrow 0$ ;
  else if  $j \leq n_{\text{only } \phi} + n_{\text{increase } \delta}$  then
     $\tilde{\delta} \leftarrow \tilde{\delta} + \delta / n_{\text{increase } \delta}$ ;
  else
     $\tilde{\delta} \leftarrow \delta$ ;
  end
  for minibatches  $(x_{i_1}, y_{i_1}), \dots, (x_{i_M}, y_{i_M})$  from  $\mathcal{D}$ ;
  do
    Compute  $\sigma_x = \tilde{\delta} \cdot \sigma_y$ ;
    Draw  $\zeta_{i_m, 1}, \dots, \zeta_{i_m, L}$  from  $\pi(\zeta_{i_m, l} | x_{i_m}, \sigma_x^2)$  for each  $m$ ;
    Draw  $\theta_1, \dots, \theta_M$  from  $q_\phi(\theta_m)$ ;
    Feedforward  $(\zeta_{i_m, l})_{m \leq M, l \leq L}$  through  $f_\theta$ ;
    Compute  $\mathcal{L}^{\text{M.C.}}(\phi, \sigma^2)$  as in (10);
    if  $j \leq n_{\text{only } \phi}$  then
      Update  $\phi$  via  $\nabla_\phi \mathcal{L}^{\text{M.C.}}(\phi, \sigma^2)$ ;
    else
      Update  $\phi, \sigma_y^2$  via  $\nabla_{\phi, \sigma_y^2} \mathcal{L}^{\text{M.C.}}(\phi, \sigma^2)$ ;
    end
  end
end

```

**Algorithm 1:** Training a neural network with EiV as described in Section 2. The algorithm uses the Deming assumption (12).

**Data:**  $x^*$  and  $\phi, \sigma_x$

**Result:** Approximation to  $m(x^*)$  and  $u(x^*)$

Sample  $\zeta_1^*, \dots, \zeta_L^*$  **from**  $\pi(\zeta_l^* | x^*, \sigma_x^2)$ ;

Sample  $\theta_1, \dots, \theta_K$  **from**  $q_\phi(\theta_k)$ ;

**for**  $k$  **in**  $1, \dots, K$  **do**

  | Feed-forward  $m_{lk} = f_{\theta_k}(\zeta_l^*)$  **for**  $l$  **in**  $1, \dots, L$ ;

**end**

Set  $m(x^*) = \frac{1}{LK} \sum_{l,k} m_{lk}$ ;

Set  $u(x^*) = \frac{1}{LK-1} \sqrt{\sum_{l,k} (m_{lk} - m(x^*))^2}$ ;

**Algorithm 2:** Computing the prediction  $m(x^*)$  and the corresponding uncertainty  $u(x^*)$  for an input  $x^*$  of an EiV model as described in Section 2.4 and using the approximation (7).

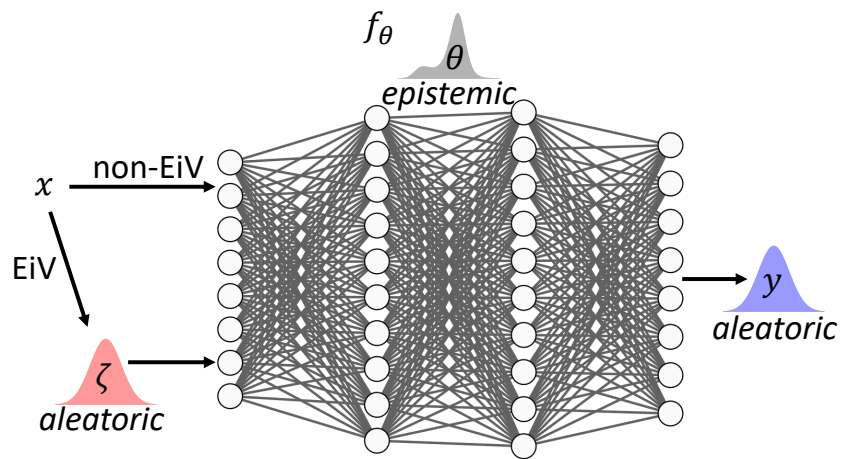


Figure 7: Illustration of the Errors-in-Variables (EiV) approach presented in this work and the method without EiV (“non-EiV”). The EiV model introduces an additional uncertainty to the input of the network that is aleatoric and, in contrast to the one linked with  $y$ , in many cases more coherent with the classical statistical view on uncertainty cf. Section 1. The network illustration was created using [17].